

Ring current instabilities excited by the energetic oxygen ions

A. P. Kakad,^{a)} S. V. Singh, and G. S. Lakhina

Indian Institute of Geomagnetism, New Panvel (West), Navi Mumbai-410 218, India

(Received 5 April 2007; accepted 7 August 2007; published online 26 September 2007)

The ring current instabilities driven by the energetic oxygen ions are investigated during the magnetic storm. The electrons and protons are considered to have Maxwellian distributions, while energetic oxygen ions are having loss-cone distribution. Dispersion relation for the quasiaelectrostatic modes with frequencies $\omega > \omega_{cp}$ (proton cyclotron frequency) and propagating obliquely to the magnetic field is obtained. Dispersion relation is studied numerically for the storm time ring current parameters and it is found that these instabilities are most prominent during intense storms when the oxygen ions become the dominant constituents of the ring current plasma. For some typical storm-time ring current parameters, these modes can produce quasiaelectrostatic noise in the range of 17–220 Hz, thus providing a possible explanation of the electrostatic noise observed at the inner boundary of the ring current during magnetic storms. Further, these modes can attain saturation electric fields of the order of 100–500 $\mu\text{V}/\text{m}$, and therefore, are expected to scatter O^+ ions into the loss-cone giving rise to their precipitation into the atmosphere, thus contributing to the ring current decay. © 2007 American Institute of Physics. [DOI: 10.1063/1.2777117]

I. INTRODUCTION

The multipoint satellite observations and modelling efforts support the idea of coupling between the high latitude ionosphere and the regions of magnetosphere. Observations from two space missions, AMPTE (Active Magnetospheric Particle Tracer Explorer) and CRRES (Combined Release and Radiation Effects Satellite), have demonstrated that the abundance of terrestrial O^+ ions in the inner magnetosphere increases quickly, as a fast response of the ionosphere to enhanced geospace activity during geomagnetic storm and substorm.¹ During the geomagnetic activity, the energetic ion flux enhancement² is more pronounced for O^+ ions than for H^+ .

The development of an intense ring current is an essential part of the geomagnetic storm. The main sources of ring current particles are the solar wind and the terrestrial ionosphere. The quiet time ring current is dominated by protons. The only other ion species that contributes substantially to the ring current is O^+ ion, which become increasingly important with the geomagnetic activity, and eventually dominates the ring current during great storms.^{3,4} It is well known that the energetic particles provide a source of free energy to excite different types of plasma instabilities. AMPTE/CCE observations indicates the presence of electromagnetic ion cyclotron (EMIC) waves most frequently in the outer magnetosphere⁵ beyond $L=7$. These waves can occur in three distinct bands below the gyrofrequencies of H^+ , He^+ , and O^+ . The excited band is controlled by the ion composition and anisotropy,^{6,7} the level of geomagnetic activity,⁸ and the location with respect to plasma pause.⁹ Thorne and Horne¹⁰ have shown that increased fluxes of O^+ ions favors the generation of waves below the oxygen gyrofrequency and damps the waves above it. The ultralow-frequency

(ULF) waves with the spectrum localized near the harmonics of the proton cyclotron frequency have been observed and verified by several satellites in the equatorial plasmasphere.^{11–14} The electrostatic ion cyclotron (EIC) waves have been observed on the auroral field lines by many satellites namely, S3-3 satellite,^{15–17} Viking,¹⁸ ISEE-1satellite,¹⁹ and Polar.²⁰ For the excitation of the EIC waves, currents, ion beams, and velocity shear have all been proposed to provide the free energy for the instability.^{21,22}

The ring current decay is mainly due to the charge exchange with exospheric neutrals, Coulomb collisions with the thermal plasma, and wave particle interactions. The enhanced charge exchange loss of ring current ions having small pitch angles²³ deepens the loss cone and increases the anisotropy of the drifting ion distributions making them more unstable to the generation of the plasma instabilities. In the ring current region a quasiaelectrostatic instability can be excited by loss-cone distribution of protons.^{24–28} Recently Singh *et al.*²⁹ have studied the quasiaelectrostatic low-frequency instabilities excited by the anisotropic O^+ ions in the ring current region. They found that the waves with frequency near the cyclotron harmonics of the oxygen ions can be excited by the anisotropic oxygen ions.

In the present paper the above work has been extended to study the obliquely propagating modes with frequencies greater than the proton cyclotron frequency. Using the energetic oxygen ions as a free energy source, we study these modes in the ring current region during the storm main phase. Ring current plasma is considered to consist of Maxwellian distributed electrons and protons, and energetic oxygen ions are having a Dory-Guest-Harris (DGH) type of distribution. In the next section, we present the theoretical model. The numerical results are discussed in Sec. III. Discussion on the application of the results to storm-time ring current is given in Sec. IV.

^{a)} Author to whom correspondence should be addressed. Electronic mail: amar@iigs.igm.res.in

II. THEORETICAL ANALYSIS

We consider the three-component plasma consisting of Maxwellian distributed electrons and background protons, and loss cone type distributed oxygen ions with the Dory-Guest-Harris (DGH) type of distributions,^{24,28-31}

$$f_o = \frac{N_o}{\pi^{3/2} J! \alpha_{\perp o}^2} \left(\frac{v_{\perp}}{\alpha_{\perp}} \right)^{2J} e^{-[(v_{\perp}^2/\alpha_{\perp}^2) + (v_{\parallel}^2/\alpha_{\parallel o}^2)]}, \quad (1)$$

where

$$\alpha_{\perp}^2 = \frac{\alpha_{\perp o}^2}{J+1},$$

$\alpha_{\parallel o} = \sqrt{2T_{\parallel o}/m_o}$, and $\alpha_{\perp o} = \sqrt{2T_{\perp o}/m_o}$ are the parallel and perpendicular thermal velocity of the oxygen ions, respectively, $J=0,1,2,3,\dots$ is the loss-cone index defining the depth of the loss cone, N_o , $T_{\parallel o}$, and $T_{\perp o}$ are the density, parallel, and perpendicular temperatures of the oxygen ions. We have assumed charged neutrality in the equilibrium state which demands that $N_e = N_{pb} + N_o$, where N_e and N_{pb} are the number densities of electrons and protons, respectively. In this analysis we have considered the electrons and protons to be isotropic. This assumption is for the sake of mathematical simplicity and to emphasize the effect of energetic oxygen ions on the excitation of waves.

In our analysis we assume the response of protons and oxygen ions to the perturbations as if they are unmagnetized ($\omega > \omega_{co}, \omega_{cpb}$) in the sense that they follow the straight line orbits. This is justified because perturbations are of much higher frequency than the cyclotron frequency of the protons and oxygen ions and, on the perturbation time scale, the ambient magnetic field does not distort their orbits significantly. Further, the electrons are treated as magnetized since the wave frequency is much smaller than the electron cyclotron frequency, i.e., $\omega \ll \omega_{ce}$. The response of the electrons is taken as fully electromagnetic, i.e., $\omega_{pe}^2/c^2k^2 \gg 1$, while protons and oxygen ions are considered to be electrostatic, i.e., $\omega_{ppb}^2/c^2k^2 \ll 1$, and $\omega_{po}^2/c^2k^2 \ll 1$. Under the above assumptions, a dispersion relation for the waves propagating obliquely to the magnetic field $\mathbf{B}_0 \parallel \mathbf{z}$ can be obtained by solving the linearized Vlasov equation along with Maxwell's equations and is written as^{24,28-31}

$$\begin{aligned} & 1 + \frac{\omega_{pe}^2}{\omega_{ce}^2} \left[\frac{1 - I_0(\lambda_e)e^{-\lambda_e}}{\lambda_e} \right] \\ & + \frac{\omega_{pe}^2 \omega_{pe}^2}{\omega_{ce}^2 c^2 k^2} \left[\frac{[I_0(\lambda_e) - I_1(\lambda_e)]e^{-\lambda_e}}{1 + \beta_e \{I_0(\lambda_e) - I_1(\lambda_e)\}e^{-\lambda_e}} \right] \\ & - \frac{k_{\parallel}^2 \omega_{pe}^2}{k_{\perp}^2 \omega^2} \frac{I_0(\lambda_e)e^{-\lambda_e}}{1 + \frac{\omega_{pe}^2}{c^2 k^2} I_0(\lambda_e)e^{-\lambda_e}} - \frac{\omega_{ppb}^2}{k_{\perp}^2 \alpha_{pb}^2} Z'(\xi_{pb}) \\ & - \frac{2\pi\omega\omega_{po}^2}{k_{\perp} k^2 \alpha_{\perp}^{2J+2}} \frac{(-1)^J}{J!} \frac{d^J}{d\mu^J} \left[\mu^{1/2} \left\{ Z'(\xi_o) + S'(\xi_o) \right. \right. \\ & \left. \left. - \frac{1}{2\sqrt{\pi}} \frac{d}{d\xi_o} (e^{-\xi_o^2} E_i(\xi_o^2)) \right\} \right] = 0, \quad (2) \end{aligned}$$

where $Z'(\xi_{pb})$ and $Z'(\xi_o)$ are derivatives of the plasma dispersion function $Z(\xi_{pb})$ and $Z(\xi_o)$ with their respective argument, $\xi_{pb} = \omega/k\alpha_{pb}$ and $\xi_o = \omega\sqrt{\mu}/k_{\perp}$.

Here,

$$Z(\xi_{pb,o}) = \frac{1}{\sqrt{\pi}} \int_{-\infty}^{\infty} \frac{e^{-t^2}}{t - \xi_{pb,o}} dt$$

is the plasma dispersion function³² and $\mu = 1/\alpha_{\perp}^2$.

$$S(\xi_o) = e^{-\xi_o^2} \int_0^{\xi_o} e^{\xi_o^2} d\xi_o$$

is known as Dawson's integral,³³

$$E_i(\xi_o^2) = \gamma + 2 \ln \xi_o + \sum_{n=1}^{\infty} \frac{\xi_o^{2n}}{n n!},$$

where $\gamma = 0.577\ 215\ 664\ 9$ is Euler's constant.

Here $\omega_{ps} = (4\pi N_s e^2/m_s)^{1/2}$, $\omega_{cs} = eB_0/cm_s$, respectively, are the plasma and cyclotron frequencies of the species s ; \ln indicates the natural logarithm, N_s and m_s are the density and mass of the species s , k is the wave number, c is the velocity of light, $\lambda_s = k_{\perp}^2 \alpha_s^2/2\omega_{cs}^2$, α_s is the thermal speed of the species s . I_0 and I_1 are the modified Bessel functions of order 0 and 1, respectively. The subscript $s=e, pb, o$ refers to electrons, protons, and oxygen ions, respectively. Equation (2) has been derived under the assumption of $k_{\parallel}^2 T_{\parallel o}/k_{\perp}^2 T_{\perp o} \ll 1$. It is interesting to note that dispersion relation (2) does not depend on oxygen ion anisotropy explicitly because of this assumption.

Expanding the plasma dispersion function in the limit $\xi_{pb}, \xi_o < 1$, and using $\omega = \omega_r + i\gamma$; $\gamma \ll \omega_r$ and neglecting the contribution from the oxygen ions to the real frequency, we obtain expressions for real frequency, ω_r , and growth rate, γ given by

$$\omega_r = \pm \sqrt{Q/P}, \quad (3)$$

$$\begin{aligned} \gamma = & - \frac{\sqrt{\pi} \omega_r^4 \omega_{pb}^2}{Q k^3 \alpha_{pb}^3} [e^{-\omega_r^2/k^2 \alpha_{pb}^2}] \\ & - \frac{2\pi \omega_r^5 \omega_{po}^2}{Q k_{\perp}^2 k^2 \alpha_{\perp}^{2J+2}} \frac{(-1)^J}{J!} \left[\frac{d}{d\mu^J} (\mu e^{-\omega_r^2 \mu k_{\perp}^2}) \right], \quad (4) \end{aligned}$$

where

$$\begin{aligned} P = & 1 + \frac{\omega_{pe}^2}{\omega_{ce}^2} \left[\frac{1 - I_0(\lambda_e)e^{-\lambda_e}}{\lambda_e} \right] \\ & + \frac{\omega_{pe}^2 \omega_{pe}^2}{\omega_{ce}^2 c^2 k^2} \left[\frac{[I_0(\lambda_e) - I_1(\lambda_e)]e^{-\lambda_e}}{1 + \beta_e \{I_0(\lambda_e) - I_1(\lambda_e)\}e^{-\lambda_e}} \right] + \frac{\omega_{ppb}^2}{k_{\perp}^2 \alpha_{pb}^2}, \quad (5) \end{aligned}$$

$$Q = \frac{k_{\parallel}^2 \omega_{pe}^2 I_0(\lambda_e) e^{-\lambda_e}}{k_{\perp}^2 \left[1 + \frac{\omega_{pe}^2}{c^2 k^2} I_0(\lambda_e) e^{-\lambda_e} \right]}. \quad (6)$$

The first term on the left-hand side of Eq. (4) represents the damping due to protons. It can be seen from the growth rate expression (4) that for $J=0$, the growth rate is negative

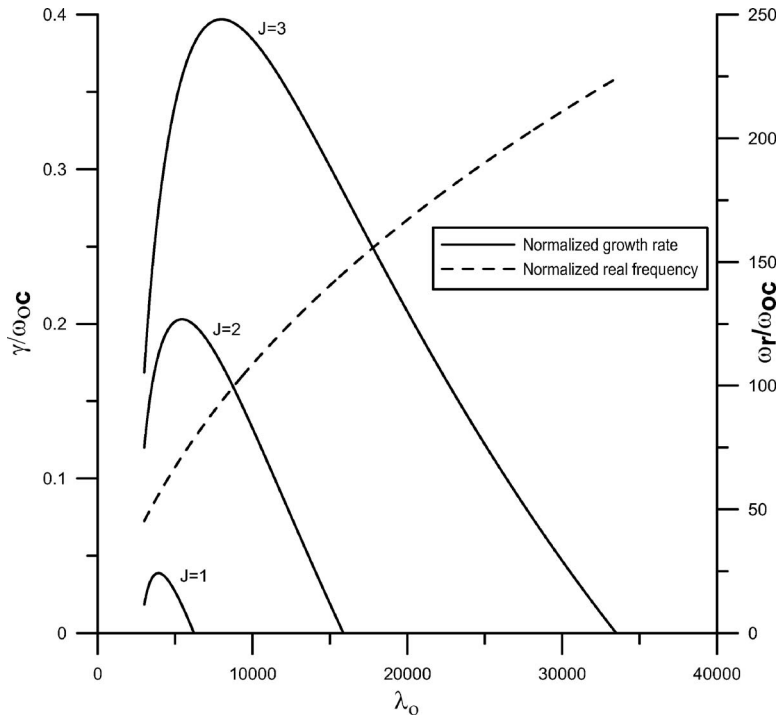


FIG. 1. The normalized real frequency ω_r/ω_{co} (- -) and growth rate (γ/ω_{co}) (—) vs normalized wave number (λ_o) for different J and the typical parameters $\omega_{pe}/\omega_{ce}=2$, $T_{\perp o}/T_e=400$, $T_{\perp o}/T_{pb}=400$, $k_{\parallel}/k=0.09$, $n_o/n_e=0.3$.

($\gamma < 0$) and the waves are damped. This is due to the fact that there is no free energy source to drive the instability.

The growth rate for $J=1$ is given by

$$\gamma = -\frac{\sqrt{\pi}\omega_r^4\omega_{pb}^2}{Qk^3\alpha_{pb}^3}[e^{-\omega_r^2/k^2\alpha_{pb}^2}] + \frac{8\pi\omega_r^5\omega_{po}^2}{Qk_{\perp}^2k^2\alpha_{\perp o}^4} \times e^{-2\omega_r^2/k_{\perp}^2\alpha_{\perp o}^2} \left[1 - \frac{2\omega_r^2}{k_{\perp}^2\alpha_{\perp o}^2}\right]. \quad (7)$$

For $J=2$ growth rate is given by

$$\gamma = -\frac{\sqrt{\pi}\omega_r^4\omega_{pb}^2}{Qk^3\alpha_{pb}^3}[e^{-\omega_r^2/k^2\alpha_{pb}^2}] + \frac{27\pi\omega_r^7\omega_{po}^2}{Qk_{\perp}^4k^2\alpha_{\perp o}^6} \times e^{-3\omega_r^2/k_{\perp}^2\alpha_{\perp o}^2} \left[2 - \frac{3\omega_r^2}{k_{\perp}^2\alpha_{\perp o}^2}\right]. \quad (8)$$

For $J=3$ growth rate is given by

$$\gamma = -\frac{\sqrt{\pi}\omega_r^4\omega_{pb}^2}{Qk^3\alpha_{pb}^3}[e^{-\omega_r^2/k^2\alpha_{pb}^2}] + \frac{256\pi\omega_r^9\omega_{po}^2}{3Qk_{\perp}^6k^2\alpha_{\perp o}^8} \times e^{-4\omega_r^2/k_{\perp}^2\alpha_{\perp o}^2} \left[3 - \frac{4\omega_r^2}{k_{\perp}^2\alpha_{\perp o}^2}\right]. \quad (9)$$

III. NUMERICAL RESULTS

We have numerically calculated the real frequency and the growth rate of these excited modes, for various ring current parameters. The normalized real frequency and growth rates are plotted against normalized wave number ($\lambda_o = k_{\perp}^2\alpha_{\perp o}^2/2\omega_{co}^2$) for different values of loss-cone index J , in Fig. 1. It shows that the normalized growth rate and the range of the excited wave numbers increase with the increase of J . This is expected here, as more deeper loss cone provides the larger amount of free energy to excite the modes

and increase their growth rate. Also it is found that the corresponding normalized real frequency increases with λ_o but remains unaffected by an increase of J . We have studied the effect of various parameters on the normalized real frequency and the growth rate of the excited modes in detail for the case of $J=1$. The variation of normalized real frequency and the growth rate γ/ω_{co} with λ_o for different values of the fractional oxygen ion density N_o/N_e is shown in Fig. 2. It is found that the peak growth rate of the excited modes increases with the increase of oxygen ion density, while the associated real frequencies and the range of unstable wave numbers decreases with an increase of N_o/N_e . Figure 3 shows that the range of unstable wavelength, normalized real frequency and the growth rates increased by the increase of ω_{pe}/ω_{ce} . It is interesting here to note that, the smaller the magnetic field, the larger the growth rate for the fixed oxygen ion concentration. The effect of k_{\parallel}/k (propagation angle) on the normalized real frequency and the growth frequency of the excited mode is shown in Fig. 4. In this case the maximum growth rate and the corresponding real frequencies of the excited waves decreases with the increase in k_{\parallel}/k values. Further it is pointed out that the range of excited wave numbers decreases with the increase of k_{\parallel}/k . The effect of oxygen ions perpendicular temperature to proton temperature ratio ($T_{\perp o}/T_{pb}$) on the excitation of the waves is shown in Fig. 5. It is found that the maximum growth rate for the excited waves increases with the increase in ($T_{\perp o}/T_{pb}$) values. It is also found that the corresponding real frequencies and the ranges of the unstable wave numbers increases with the increase of ($T_{\perp o}/T_{pb}$).

IV. DISCUSSION AND APPLICATION

The model presented in this paper deals with the excitation of quasiaelectrostatic instabilities with frequencies

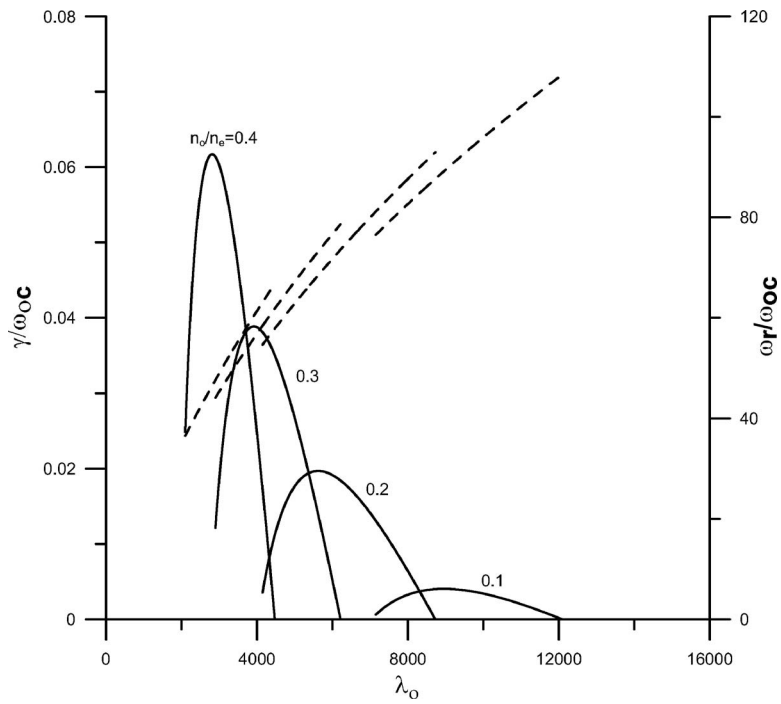


FIG. 2. Variation of normalized real frequency ω_r/ω_{oc} (- - -) and growth rate γ/ω_{oc} (—) vs normalized wave number (λ_o) for $J=1$, and different number density ratio. Other parameters are the same as in Fig. 1.

greater than the proton cyclotron frequency in the ring current region. For the complete numerical computations, we have used the storm time ring current parameters to calculate the growth rate of the excited mode from Eq. (4) for different values of J . The calculated values of the maximum growth rate and their corresponding real frequencies for $J=1, 2, 3$ are found to be (0.04 Hz, 17 Hz), (0.1 Hz, 58 Hz), and (0.4 Hz, 220 Hz), respectively. The corresponding perpendicular and parallel wavelength range is calculated to be $\sim 5\text{--}20$ km and $\sim 50\text{--}180$ km, respectively, for $T_{\perp o} = 30$ keV, $B_0 = 500$ nT ($L \sim 4$) (here B_0 and $T_{\perp o}$ are taken

from Thorne and Horne¹⁰). It is found that the growth rate of the excited modes increases with the increase in the loss cone depth and oxygen ion concentration. During the main phase of the magnetic storm, population of energetic O^+ ions increases substantially.³ Therefore, magnetic storm main phase provides a favorable situation for the excitation of the modes studied here.

Following Coroniti *et al.*,²⁴ we assume that as the unstable modes grow, they will start trapping the O^+ ions in the wave field. The process will continue until the linear growth

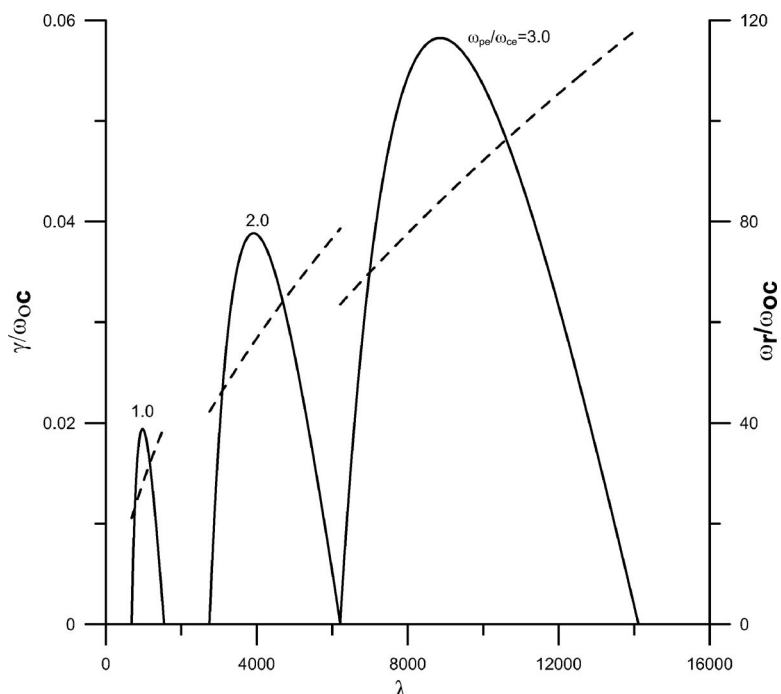


FIG. 3. Variation of normalized real frequency ω_r/ω_{oc} (- - -) and growth rate γ/ω_{oc} (—) vs normalized wave number (λ_o) for $J=1$, and the various values of electron plasma frequency $\omega_{pe}/\omega_{ce}=1, 2, 3$. The other parameters are the same as in Fig. 1.

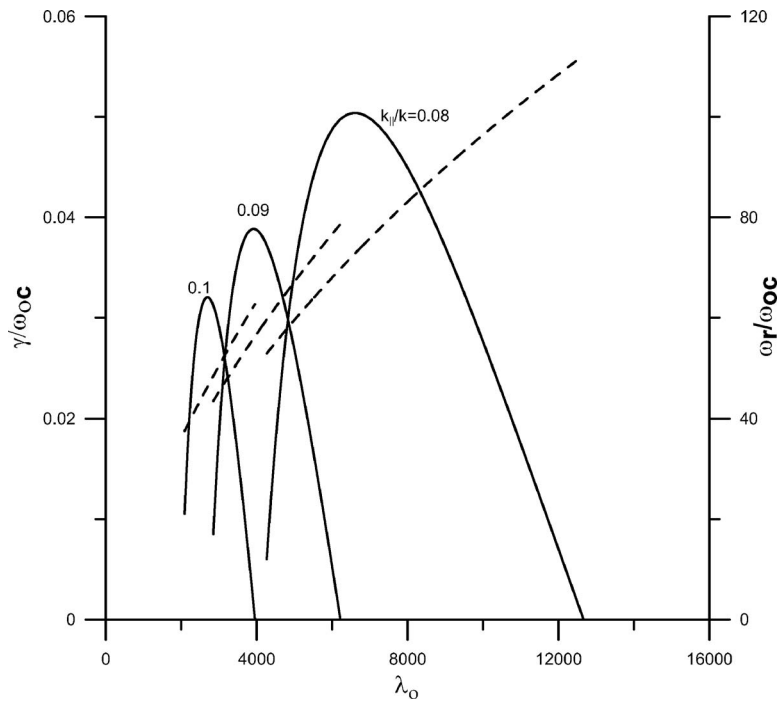


FIG. 4. Variation of normalized real frequency ω_r/ω_{oc} (- - -) and growth rate γ/ω_{oc} (—) vs normalized wave number (λ_o) for $J=1$, and various values of $k_{||}/k=0.08, 0.09, 0.1$. The other parameters are the same as in Fig. 1.

rate equals the trapping frequency of the O^+ ions in the saturated wave field,

$$\omega_t = \sqrt{\frac{ekE_s}{m_o}}, \tag{10}$$

where E_s is the saturated electric field of the wave. Therefore, by considering the modes are stabilized by the trapping of oxygen ions by the waves when their amplitude becomes

large, the saturation electric field for the excited mode is given by

$$E_s \approx \frac{m_o \gamma^2}{e k}. \tag{11}$$

Using Eq. (4) in Eq. (11) we get the saturation electric field as

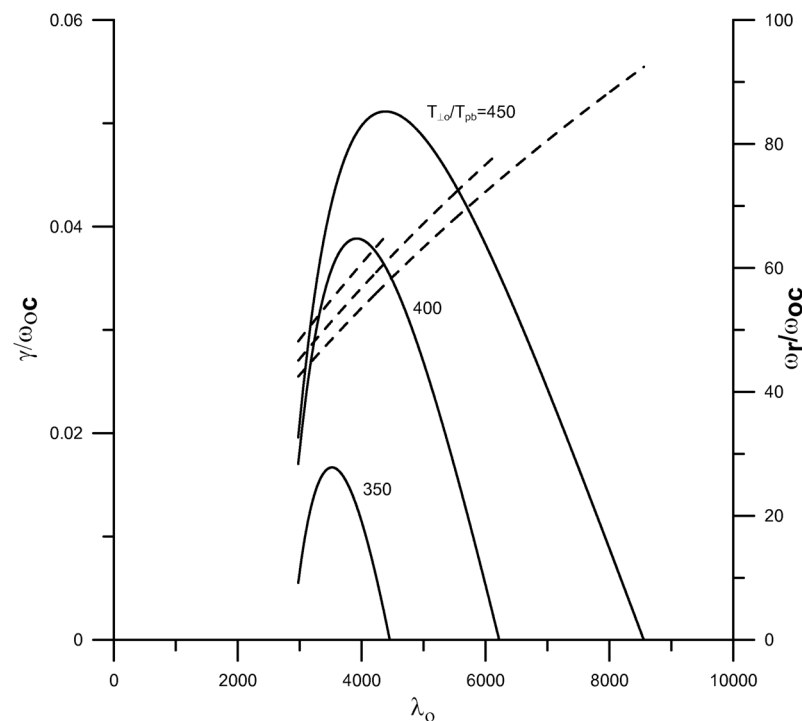


FIG. 5. Variation of normalized real frequency ω_r/ω_{oc} (- - -) and growth rate γ/ω_{oc} (—) vs normalized wave number (λ_o) for $J=1$, and $T_{\perp o}/T_{pb}=350, 400, 450$, respectively, shown as curves 1, 2, and 3. The other parameters are the same as in Fig. 1.

$$E_s = \frac{4\pi^2 m_o \omega_r^{10} \omega_{po}^4}{ek^5 k_{\perp}^4 Q^2 \alpha_{\perp}^{4(j+1)}} \left\{ \frac{(-1)^j}{J!} \left[\frac{d}{d\mu^j} (\mu e^{-\omega_r^2 \mu k_{\perp}^2}) \right] \right\}^2. \quad (12)$$

Using the ring current parameters, the range of the saturation electric field E_s of the excited mode is calculated to be 0.3–5 $\mu\text{V/m}$, 0.2–115 $\mu\text{V/m}$, and 0.12 $\mu\text{V/m}$ –0.4 mV/m for $J=1, 2$, and 3, respectively.

For the combined effect of anisotropy and the loss cone distribution, we can construct a pitch angle diffusion coefficient, D , given by^{28,29}

$$D = \frac{(\Delta v_{\perp})^2}{2 \Delta t}, \quad (13)$$

where $\Delta v_{\perp} = eE_s \Delta t / m_o$ and Δt is the wave-particle correlation time. Since $\gamma \sim (ekE_s / m_o)^{1/2}$, and assuming $\Delta t \approx \gamma^{-1}$, then D is given by

$$D \approx \frac{\gamma^3}{2k^2}. \quad (14)$$

The range of diffusion coefficients for $J=1, 2, 3$ are found to be of the order of 4.62×10^5 – $4.03 \times 10^7 \text{ cm}^2/\text{s}^3$, 1.74×10^5 – $3.9 \times 10^9 \text{ cm}^2/\text{s}^3$ and 8.2×10^4 – $2.1 \times 10^{10} \text{ cm}^2/\text{s}^3$, respectively. Corresponding diffusion time for an oxygen ion to reach the loss cone is calculated to be in the range of 4.5×10^7 – $4 \times 10^9 \text{ s}$, 4.6×10^5 – 10^{10} s , and 8.6×10^4 – $2.2 \times 10^{10} \text{ s}$ for $J=1, 2$, and 3, respectively. Electromagnetic ion cyclotron (EMIC) waves are known to scatter both the ring current protons and oxygen ions and therefore, are responsible for significant precipitation loss of ring current particles into the atmosphere. Jordanova *et al.*,³⁴ calculated the bounced averaged Coulomb diffusion coefficients for 150 eV ring current ions colliding with the different plasmaspheric species at $L=2.5$. They found the diffusion coefficients to be in the range of $\sim 10^{-7}$ – 10^{-9} s^{-1} , i.e., the diffusion time is in the range of $\sim 10^7$ – 10^9 s . In our model we find that for the anisotropic index ($J=1, 2, 3$) the diffusion time for an oxygen ion is in the range of $\sim 10^5$ – 10^{10} s . This shows that, for the certain parametric range, the diffusion rate of quasiaelectrostatic waves may become equal or greater than the diffusion rate of EMIC waves and may contribute to fast decay of ring current particles.

The occurrence of intense low-frequency (20–500 Hz) electrostatic noise bursts at the inner boundary of the proton ring current during the magnetic storm of 16–17 December 1971 has been reported by Anderson and Gurnett.³⁵ However, relatively less intense waves below 20 Hz have also been observed. They have suggested that this electrostatic noise may be responsible for the pitch angle scattering and loss of ring current protons from the region near the plasma pause boundary during the storm. Furthermore, they have suggested a possibility of occurrence of low-frequency noise related to the electrostatic instability described by Coroniti *et al.*²⁴ Recently, Singh *et al.*²⁸ studied the obliquely propagating low-frequency quasiaelectrostatic waves ($\omega < \omega_{cp}$) generated by the anisotropic oxygen ions. They found that the growth rate of these excited waves decreases with the increase of the anisotropic index. Also in another study of Singh *et al.*,²⁵ the obliquely propagating modes with frequen-

cies near the harmonics of oxygen ion cyclotron frequency were found to become unstable due to pressure anisotropy of the energetic oxygen ions. It is interesting to note that for the parameters considered here, the low-frequency modes (frequency < proton cyclotron frequency) discussed by Singh *et al.*^{28,29} will also be excited along with the high-frequency (> proton cyclotron) modes. However, the low-frequency modes have much smaller growth rates and would take a longer time to saturate. It is difficult to assess how much free energy would go into exciting the low-frequency modes. Further, we have assumed nonlinear trapping of oxygen ions by the wave field as the main saturation mechanism. This assumption will work fine if there is a single large amplitude wave. Since the growth rate peaks are quite broad there is a possibility that several modes with comparable amplitudes could be excited. In that case it would be more appropriate to calculate the saturation by the quasilinear diffusion theory or resonance broadening theory. This is beyond the scope of this paper. Therefore, the estimates for the saturation electric field given by Eq. (12) can be taken as the upper limit. It is emphasized here that our mechanism may be relevant for explaining the low frequency part of the noise observed by Anderson and Gurnett.³⁵

We would like to point out that although the main component of the electric field, \mathbf{E}_L , associated with the modes would be in the direction of the wave vector \mathbf{k} , there will be a small component of the electric field transverse the wave vector, $\mathbf{E}_T = \mathbf{E} - \mathbf{E}_L$ due to the electromagnetic effects on electrons. The transverse electric field would give rise to a fluctuating magnetic field \mathbf{B}_Z along the Z-direction given by^{27,36}

$$B_Z = \frac{ck_{\perp} E_T}{\omega} = \frac{10^{-2}}{3} \left(\frac{2\lambda_o c^2 \omega_{co}^2}{\alpha_{\perp o}^2 \omega^2} \right)^{1/2} \left(\frac{E_T}{E} \right) E_s, \quad \text{nT}. \quad (15)$$

We have $\alpha_{\perp 0} = 6 \times 10^5 \text{ m/s}$ (corresponding to $T_{\perp 0} = 30 \text{ keV}$), $E_T/E = 10^{-3}$ – 10^{-2} . Using these parameters in Eq. (15), the maximum fluctuating magnetic field B_Z is found to be in the range of 0.3–40 pT for $J=1$ –3.

During geomagnetic storms the source of free energy for the wave excitation is greatly enhanced due to an increase of concentration of energetic O^+ ions in the ring current region. Both the temperature anisotropy as well as the loss cone is expected to increase when the energetic O^+ ions are pushed towards lower L values. These factors lead to the excitation of different kinds of waves, including the waves with frequencies greater than the proton cyclotron frequencies in the ring current region during magnetic storm. It is known that the role of the ionospheric oxygen ions in the evolution of intense magnetic storms is twofold. The explosive ionospheric oxygen ion feeding of the magnetosphere may cause a rapid enhancement of the ring current at storm maximum³⁷ and induce an equally rapid initial ring current decay.³ Furthermore, oxygen ion loaded ring current can affect the charge exchange process which is considered as a major process for the ring current decay. The electromagnetic ion cyclotron waves are believed to be important for the wave particle interaction in the ring current region.¹⁰ The modes studied here can interact with the ring current particles.

These interactions can allow efficient energy transfer between different ions under certain conditions which produce large growth rates and high saturation electric field. Further, these excited waves may scatter the ring current particles into the loss cone, leading to their precipitation in the ionosphere. This would contribute to the decay of the ring current because of the loss of ring current particles. For example, considering the peak diffusion time for the $J=3$ case, the O^+ ions would precipitate into their loss-cone leading to the ring-current decay of ~ 24 h. Under the conditions of higher J (i.e., $J \geq 4$) which could exist during intense magnetic storms when the ring-current is pushed to lower L values, the ring-current decay could be as short as several hours.

ACKNOWLEDGMENTS

This work was done under the CAWSES-India project, "Boundary layer waves and ring current dynamics." A.P.K. and S.V.S. would like to thank ISRO, Bangalore for financial support. G.S.L. would like to thank the Council of Scientific and Industrial Research, Government of India, for the support under the Emeritus Scientist Scheme.

- ¹I. A. Daglis and W. I. Axford, *J. Geophys. Res.* **101**, 5047, DOI:10.1029/95JA02592 (1996).
- ²M. Nose, A. T. Y. Lui, S. Ohtani, B. H. Mauk, R. W. McEntire, D. J. Williams, T. Mukai, and K. Yumoto, *J. Geophys. Res.* **105**, 7669, DOI:10.1029/1999JA000318 (2000).
- ³I. A. Daglis, *Magnetic Storms, Geophysical Monographs Series*, edited by B. T. Tsurutani, W. D. Gonzalez, Y. Kamide, and J. K. Arballo (American Geophysical Union, Washington, D.C., 1997), Vol. 98, p. 107.
- ⁴I. A. Daglis, *EOS Trans. Am. Geophys. Union* **24**, 145 (1997).
- ⁵B. J. Anderson, K. Takahashi, R. E. Erlandson, and L. J. Zanetti, *Geophys. Res. Lett.* **17**, 1853 (1990).
- ⁶J. U. Kozyra, T. E. Cravens, A. F. Nagy, E. G. Fontheim, and R. S. B. Ong, *J. Geophys. Res.* **89**, 2217 (1984).
- ⁷R. B. Horne and R. M. Thorne, *J. Geophys. Res.* **99**, 17259, DOI:10.1029/94JA01259 (1994).
- ⁸T. Bräysy, K. Mursula, and G. Marklund, *J. Geophys. Res.* **103**, 4145, DOI:10.1029/97JA02820 (1998).
- ⁹B. J. Fraser and T. S. Nguyen, *J. Atmos. Sol.-Terr. Phys.* **63**, 1225 (2001).
- ¹⁰R. M. Thorne and R. B. Horne, *J. Geophys. Res.* **102**, 14155, DOI:10.1029/96JA04019 (1997).
- ¹¹C. T. Russell, R. E. Holzer, and E. J. Smith, *J. Geophys. Res.* **75**, 755 (1970).
- ¹²W. L. Taylor, B. Parady, and L. J. Cahil, Jr., *J. Geophys. Res.* **80**, 1271 (1975).
- ¹³D. A. Gurnett, *J. Geophys. Res.* **81**, 2765 (1976).
- ¹⁴P. M. Kinter and D. A. Gurnett, *J. Geophys. Res.* **82**, 2314 (1977).
- ¹⁵P. M. Kinter, M. Kelley, and F. Mozer, *Geophys. Res. Lett.* **5**, 139 (1978).
- ¹⁶P. M. Kinter, M. C. Kelley, R. D. Sharp, A. G. Ghielmetti, M. Temerin, C. Cattell, P. F. Mizera, and J. F. Fennel, *J. Geophys. Res.* **84**, 7201 (1979).
- ¹⁷M. Temerin, M. Woldorff, and F. S. Mozer, *Phys. Rev. Lett.* **43**, 1941, DOI:10.1103/PhysRevLett.43.1941 (1979).
- ¹⁸M. Andre, H. Koskinen, G. Gustafsson, and R. Lundin, *Geophys. Res. Lett.* **14**, 463 (1987).
- ¹⁹C. A. Cattell, F. S. Mozer, I. Roth, R. R. Anderson, R. C. Elphic, W. Lennartsson, and E. Ungstrup, *J. Geophys. Res.* **96**, 11421 (1991).
- ²⁰F. S. Mozer, R. Ergun, M. Temerin, C. Cattell, J. Dombeck, and J. Wygant, *Phys. Rev. Lett.* **79**, 1281 (1997).
- ²¹G. S. Lakhina, *J. Geophys. Res.* **92**, 12161 (1987).
- ²²G. Ganguli, Y. C. Lee, and P. J. Palmadesso, *Phys. Fluids* **31**, 823 (1988).
- ²³J. M. Cornwall, *J. Geophys. Res.* **82**, 1188 (1977).
- ²⁴F. V. Coroniti, R. W. Fredricks, and R. White, *J. Geophys. Res.* **77**, 6243 (1972).
- ²⁵W. Bernstein, B. Hultqvist, and H. Borg, *Planet. Space Sci.* **22**, 767 (1974).
- ²⁶G. S. Lakhina, *Planet. Space Sci.* **24**, 609 (1976).
- ²⁷K. G. Bhatia and G. S. Lakhina, *Earth Planet. Sci. Lett.* **89**, 99 (1980).
- ²⁸S. V. Singh, A. P. Kakad, R. V. Reddy, and G. S. Lakhina, *J. Plasma Phys.* **70**, 613 (2004).
- ²⁹S. V. Singh, A. P. Kakad, and G. S. Lakhina, *Phys. Plasmas* **12**, 012903 (2005).
- ³⁰R. C. Davidson, N. T. Gladd, C. S. Wu, and J. D. Huba, *Phys. Fluids* **20**, 301 (1977).
- ³¹K. G. Bhatia and G. S. Lakhina, *Planet. Space Sci.* **25**, 833 (1977).
- ³²B. D. Fried and S. D. Conte, *The Plasma Dispersion Function* (Academic, New York, 1961).
- ³³M. Abramowitz and I. A. Stegun, *Handbook of Mathematical Functions with Formulas, Graphs, and Mathematical Tables* (Dover, New York, 1972), p. 298.
- ³⁴V. K. Jordanova, L. M. Kistler, J. U. Kozyra, G. V. Khazanov, and A. F. Nagy, *J. Geophys. Res.* **101**, 111, DOI:10.1029/95JA02000 (1996).
- ³⁵R. R. Anderson and D. A. Gurnett, *J. Geophys. Res.* **78**, 4756 (1973).
- ³⁶D. S. Lemons and S. P. Gary, *J. Geophys. Res.* **82**, 2337 (1977).
- ³⁷Y. Kamide, N. Yokoyama, W. Gonzalez, B. T. Tsurutani, I. A. Daglis, A. Brekke, and S. Masudha, *J. Geophys. Res.* **103**, 6917, DOI:10.1029/97JA03337 (1998).